Sensors & Actuators: B. Chemical 374 (2023) 132769

Contents lists available at ScienceDirect

Sensors and Actuators: B. Chemical

journal homepage: www.elsevier.com/locate/snb

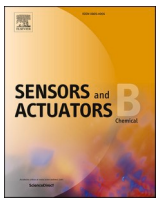

Bacterial concentration and detection using an ultrasonic nanosieve within a microfluidic device

Bryan Ang [a,d], Ruhollah Habibi [a], Ciaren Kett [b], Wai Hoe Chin [b], Jeremy J. Barr [b], Kellie L. Tuck [c,*], Adrian Neild [a,*], Victor J. Cadarso [a,d,**]

[a] Department of Mechanical and Aerospace Engineering, Monash University, Clayton 3800, VIC, Australia
[b] School of Biological Sciences, Monash University, Clayton 3800, VIC, Australia
[c] School of Chemistry, Monash University, Clayton 3800, VIC, Australia
[d] Centre to Impact Antimicrobial Resistance, Monash University, Clayton 3800, VIC, Australia

ARTICLE INFO

Keywords:
Surface acoustic waves
Nanosieve
Microfluidics
Bacteria detection
Ultrasonics
Acoustic radiation force
Bacteria concentration

ABSTRACT

Standard methods, such as plate counting, to detect bacteria in samples where only small volumes and low concentrations are available, will result in a negative detection, unless additional enriching steps, such as culturing, are used. However, these are laborious and time consuming, which may prevent their effective application to time sensitive situations, for example in clinical settings or for food quality control. Microfluidic concentration of bacterial cells can address this issue, enabling accurate detection and quantification in low abundance samples even when only small sample volumes are used. In this work we use a packed bed of microparticles trapped in a microfluidic chip, that are activated with surface acoustic waves to periodically concentrate and detect bacteria from sample volumes below 10 μL. We demonstrate a bacterial capturing efficiency of 99% and further demonstrate that the concentrated bacteria can be recovered with an 80% efficiency. This highly concentrated recovered sample can then be successfully used in standard methods, such as plate counting and PCR, for the detection of the bacteria using just 1 μL of sample without the need for a culture-based enrichment process. When integrating our ultrasonic nanosieve with fluorescence sensing, it is possible to achieve rapid detection of a wide range of bacteria concentrations. The device enables the fluorescence detection of bacteria concentration of 4×10^5 CFU/mL in only 15 s and achieved a limit of detection of 3.25×10^2 CFU/mL with just 32 min of ultrasonic actuation, requiring only 10 μL of sample. These results demonstrate that our device offers a scalable, portable, and affordable method for the monitoring of low bacterial concentration using small sample volumes.

1. Introduction

Early detection of bacteria, especially when sample volumes are limited and the bacteria concentrations are low (~10^2 colony forming units (CFU)/mL and lower), is important for the diagnoses of diseases [1,2], as well as an early indicator for contamination in food production lines [3,4]. The most common approach for detection of bacterial cells typically requires a culture-based enrichment step [5] and is often paired with standard plate counting for enumeration of bacteria colonies on agar plates for the prediction of initial bacteria concentrations. Although these culture-based methods are inexpensive and relatively straightforward, protocols can be excessively time-consuming [6–8]. In addition to that, plating standards depict that large plating volumes between 100 and 200 μL [9] are required for enumeration. Whilst necessary, for samples with low bacteria populations it is not always achievable due to small volumes of precious samples. In order to reduce analysis times of samples with low initial abundance and volume, methods that do not require culture-based enrichment have been developed. These can include molecular-based techniques such as polymerase chain reaction (PCR) [10,11], in situ hybridization techniques (ISH) [12,13], or selective immunological assays, such as enzyme-linked immunosorbent assay (ELISA) [14]. However, these methods require expensive biomolecules, bulky equipment, and highly skilled personnel, making operation outside the laboratory environment extremely

* Corresponding authors.
** Corresponding author at: Department of Mechanical and Aerospace Engineering, Monash University, Clayton 3800, VIC, Australia.
E-mail addresses: kellie.tuck@monash.edu (K.L. Tuck), adrian.neild@monash.edu (A. Neild), victor.cadarso@monash.edu (V.J. Cadarso).

https://doi.org/10.1016/j.snb.2022.132769
Received 19 July 2022; Received in revised form 27 September 2022; Accepted 28 September 2022
Available online 3 October 2022

challenging, especially within resource-limited settings [10–14]. Furthermore, when processing low target concentrations (<100 cells) a sample enrichment step is often still needed [15–19]. Advanced molecular imaging techniques such as surface-enhanced Raman scattering (SERS) have also been developed for visualization and quantitative characterization of cells, however, SERS imaging techniques can damage biological samples and require expensive high-resolution and high-speed imaging equipment [20].

Microfluidic biosensors have emerged as favorable candidates for rapid concentration and detection of bacteria due to their small size, high sensitivity, and low sample volume requirement [21]. Advanced separation and detection strategies include the use of functionalized surfaces or modified magnetic nanoparticles (MNPs) for antibody-antigen [22–25] or aptamer interactions [26–29]. High affinity and specificity aptamers have been integrated with quartz crystal microbalance sensors [27,28] and surface plasmon resonance [29] sensors for sensitive detection of bacteria in food products. However, these methods are multi-stepped techniques that require between 30 min and several hours for antibody/aptamer immobilization and for bacteria to bind to the MNPs, even before magnetic separation, washing, and detection steps can occur, making continuous detection and long-term reusability difficult [30].

Other popular enrichment strategies include electrophoretic (EP) [31,32] and dielectrophoretic (DEP) [32] techniques which exploit the polarizable particle dipoles by means of an external electric field for separation from other particles with different dielectric properties. Both methods are critically limited for live cells analysis due to their dependence on cell polarizability and their need for low conductivity media for separation, which may disrupt cell physiology [33,34]. An alternative, and biocompatible [35–37], method of external excitation of a microfluidic volume is acoustic actuation.

Acoustofluidic approaches have been developed for the manipulation of particles [38] and cells [39–41] with a high degree of accuracy. Acoustic actuation generates three key types of forces, the acoustic radiation force which acts to migrate particles to certain locations within a sound field, acoustic streaming which is the swirling motion of the fluid and acts to drag particles with the flow, and Bjerknes force which is the force generated on one particle by another in its close proximity [42,43]. In recent works [44–47], a sound wave activated nanosieve (SWANS) was developed to minimize drag-induced streaming by exploiting the Bjerknes forces created between a packed bed of microparticles and smaller particulate matter flowing through it. The result was a system capable of capturing exosomes and nanoparticles. However, the volumetric flow rates achieved to date [46] (only 0.1 μL/min) are low, and this is particularly detrimental when preconcentrating samples with low initial concentrations of analyte.

In this work, we utilize the ultrasonic nanosieve (i.e. SWANS) system for the concentration of the bacterium *Escherichia coli* from low concentration samples (~10^2 CFU/mL) and small sample volumes (10 μL or less) to enable detection in conventional techniques, such as plate counting and PCR and demonstrate rapid fluorescence detection capability in-chip. New electrodes were designed to increase efficiency and effectively triple the working flow rate, up to 0.3 μL/min at a much lower power regime (over 10-fold decrease), whilst still maintaining high capture efficiency of 99%. This novel system enabled the concentration of bacteria into a 1 μL highly concentrated solution that can be recovered and used for plate counting and PCR. It enabled a 7-fold sample enrichment starting from concentrations as low as 5.5×10^2 CFU/mL. This method was used to validate the capabilities of our device to increase bacterial concentrations in limited-volume samples. Rapid detection and quantification of bacteria were demonstrated by means of fluorescence imaging for concentrations ranging from ~10^2 to 10^5 CFU/mL. The system exhibited a limit of detection (LOD) of 3.25×10^2 CFU/mL when concentrating samples for just 32 min (requiring just 10 μL of initial sample), and detection of higher concentrations (~10^3 CFU/mL) could be achieved in just 4 min without any additional step and requiring only 1.2 μL. These results, combined with the strong upscaling potential and the ease to operate, demonstrate the capability of this device for early bacteria detection and monitoring in point of care applications.

2. Experimental section

2.1. Materials and instrumentation

A schematic of the system for bacteria concentration with the ultrasonic nanosieve is shown in Fig. 1. It consists of a polydimethylsiloxane (PDMS) fluid channel across which a row of pillars creates a physical barrier. This barrier impedes the flow of microparticles such that a dense packed bed is created. Two sets of electrodes are deposited on a piezoelectric substrate to form a pair of interdigital transducers (IDTs), capable of creating counter-propagating surface acoustic waves. These surface waves couple into the fluid within the channel and resonate the 15 μm polystyrene microparticles that form the packed bed at a resonance frequency of 70 MHz. Characterization of the system was done using fluorescent-stained *E. coli* cells.

2.2. Interdigital transducers

The performance of the straight IDT configuration demonstrated in this work was compared against the broadband chirped IDTs used in previous work [44–47]. The chirped IDT had 35 finger pairs and surface acoustic wavelengths in the range from 20 to 70 μm, while the straight IDT had 26 finger pairs and created an acoustic wavelength fixed at 51 μm. Both IDTs had an aperture, or width, of 1 mm. For all device characterization, the IDTs were excited at 70 MHz, corresponding to the resonance frequency of the 15 μm polystyrene microparticles [46]. The IDTs were patterned on a piezoelectric base substrate, lithium niobate ($LiNbO_3$) 128° Y-cut wafer (Precision Micro-Optics), with standard UV photolithography using a positive photoresist (AZ1512HS, Micro-Chemicals). Metals deposited on the IDTs comprised of a sequential deposition of a base adhesion layer of 10 nm of Cr, a bulk conductive layer of 200 nm of Au, and a top adhesion layer 10 nm of Cr, using electron beam evaporation (Intlvac Nanochrome II E-beam), followed by lift-off with acetone. After lift-off, 300 nm of silicon dioxide was deposited via electron beam evaporation for electrical insulation.

2.3. PDMS fluid channel

The microchannel was designed with a height of 32 μm and a width of 94 μm to accommodate a uniform, dense packed bed of 15 μm microparticles. As Bjerknes forces decay with increasing distance from the microparticles, bacteria must pass close to them. Hence, the channel height was designed to be slightly over two microparticle diameters, minimizing the distance from the microparticles to the upper and lower channel boundaries and so maintaining a high capturing efficiency. The silicon mold used to fabricate PDMS microchannels, was patterned with UV lithography using negative photoresist (SU-8 3005, Micro-Chemicals). 5 μm of SU-8 was used as an etch-mask for deep reactive ion etching (DRIE) for a channel depth of 32 μm. The PDMS device, cured with polymer base to curing agent ratio of 5:1 was bonded to $LiNbO_3$ using air plasma treatment (Harrick Plasma, PDC-32 G).

2.4. Microparticle packed bed

Polystyrene microparticles (10% w/v PS/DVB Microspheres, EPRUI Biotech), used to create the packed bed were 15 μm in diameter and diluted to a working concentration of 0.1% w/v, were injected using a syringe pump (Legato 100, KD Scientific) into the microchannel.

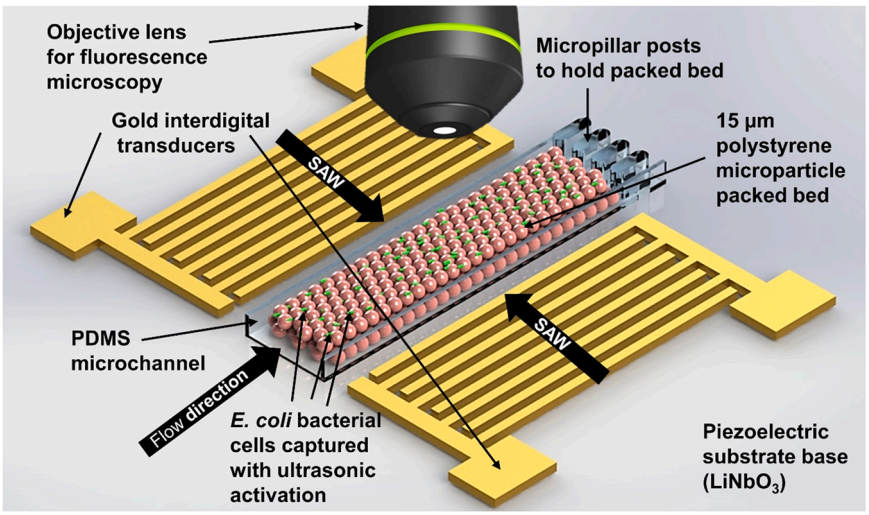

Fig. 1. Device overview showing the ultrasonic nanosieve consisting of a resonating 15 μm polystyrene microparticle packed bed capturing bacterial cells using a standing surface acoustic wavefield generated from two opposing gold straight IDTs patterned on a piezoelectric substrate ($LiNbO_3$).

2.5. Surface treatment

To reduce protein adsorption and adhesion of bacterial cells to the PDMS channel walls and the polystyrene microparticles, poloxamer 407 (Pluronic F-127, Sigma-Aldrich) was used for surface treatment [48]. 1% w/v of Pluronic F-127 in Milli-Q water was injected at 1 μL/min with a syringe pump (Legato 100, KD Scientific) into the microchannel after loading of the microparticles for 1 h, followed by a Milli-Q water wash for 1 h. Lastly, sodium chloride and magnesium sulfate buffer (SM buffer) was introduced for 1 h to remove any Milli-Q water within the channel before the bacteria sample is introduced into the microfluidic device. All surface treatments were done at room temperature.

2.6. Preparation of bacteria samples

A colony of *E. coli* DH5α cells were incubated in a 14 mL Falcon tube with 5 mL of lysogeny broth (LB) in a shaker kept (OM11 Orbital Shaking Incubator, Ratek) at 37 °C at 200 RPM overnight. The concentration of bacteria from the overnight culture is confirmed to be within the range of 4×10^8 CFU/mL to 6×10^8 CFU/mL using a spectrophotometer (C08000 cell density meter, Biowave) at optical density of 1.40 at 600 nm (OD_{600}). 1 mL of the overnight suspension was then centrifuged (Eppendorf MiniSpin) at 13,400 RPM for 1 min. The supernatant was then replaced with SM buffer pH 7.6, and the washing step was repeated twice to remove dead cells and other cellular debris. After the three washes, the sample was diluted to the target concentration and kept on ice to reduce proliferation and maintain initial cell viability until experiments began.

2.7. Fluorescence staining of bacteria

The bacterial samples were stained with a fluorescent nucleic acid stain, Syto-9 (L7012, BacLight Live/Dead Assay, ThermoFisher). Cell staining was only done for cell quantification during IDT characterization. It is important to note that unstained cells were used for experiments involving culture plating (due to stain cytotoxicity) and qPCR (potential inhibition). To test for viability of the cells, a counterstain of propidium iodide (red fluorescence) was used to determine the number of dead cells in comparison to the total cell count seen from Syto-9 (green fluorescence).

2.8. Culture plating and colony counting

Culture plating and colony counting were conducted to determine the degree of bacterial enrichment using microfluidic ultrasonic concentration, from undetected low concentrations to above the LOD of 1×10^3 CFU/mL (when using small plating volumes of 1 μL) for traditional colony counting. The plating volume was 1 μL for all replicates (N = 3–5), which were plated onto Petri dishes with LB agar. The plating volume was correlated to the throughput of the microfluidic device, with an optimum flow rate of 0.3 μL/min. The culture plates were incubated overnight at 37 °C, and the individual colonies were counted to determine the concentration of bacteria within the collected samples before, during, and after ultrasonic exposure. Control samples without ultrasonic activation of the same fluid volume were also plated for comparison.

2.9. Quantitative PCR

Bacterial genomic DNA for qPCR standards was extracted from an *E. coli* overnight culture using the GenElute Bacterial Genomic DNA Kit (Sigma-Aldrich). The culture was diluted 1:50 in 20 mL LB and incubated shaking at 37 °C for 1 h. 1.5 mL of this culture was pelleted and washed three times with 1 x PBS (OmniPur, Calbiochem). CFU plating was performed to determine live bacteria concentration and DNA extracted following kit instructions. A 10-fold dilution series was performed on the DNA sample in UltraPure™ Water (Invitrogen) to obtain a standard curve. All qPCR runs were performed on the Lightcycler 480 II (Roche) using LightCycler 480 SYBR Green I Master kit (Roche). Primers and protocols used were based on previous literature [49]. Forward: 5'-GCTACAATGGCGCATACAAA-3' Reverse: 5'-TTCATGGAGTCGAGTTGCAG-3'for amplification of the 16 S rRNA gene. All reactions final volume 20 μL: 7 μL water (from kit), 1 μL each primer (0.5 μM), 10 μL SYBR Green I Master mix, 1 μL template. Thermal cycling protocol-initial denaturation 10 min at 95 °C and 40 cycles of 10 s at 95 °C, 10 s at 60 °C and 10 s at 72 °C.

2.10. Experimental set-up

The microfluidic device was connected to a RF signal generator (SMC100A, Rhode & Schwarz, Germany) and amplifier (Amplifier Research, 25A250A) to generate a surface acoustic wave by application of an oscillating electrical signal to the IDTs. The IDTs were connected via SMA cables and spring-loaded pins held in a custom 3D-printed

device holder. The microfluidic device was mounted on top of a custom cooling set-up consisting of a Peltier cooler (Jaycar Module ZP9102). The device was cooled and maintained at 20 °C ± 5 °C. Images were taken using a high-speed digital camera (acA1920–150 μm, Basler) set to 50 frames/s, which was mounted on an upright microscope (BX43, Olympus). Fluorescent band-pass light filters (Edmund Optics, USA) were used to cover the fluorescent light excitation and emission wavelengths corresponding to that of Syto-9 (483 nm/503 nm).

2.11. Data analysis

The images captured from fluorescence imaging were analyzed using ImageJ. Macros were written for batch image processing of fluorescent cell counting at locations upstream and downstream of the packed bed. The capture efficiency was calculated from the difference between the number of cells entering the packed bed and the number of cells leaving the packed bed during ultrasonic activation. The release efficiency was calculated from the difference between the number of cells captured within the packed bed and the number of cells leaving the packed bed after turning off ultrasonic activation.

3. Results and discussions

The operation sequence of the ultrasonic nanosieve for bacterial concentration consists of four steps, which are loading of microparticles, introduction of stained bacterial cells, ultrasonic capture of bacteria within the packed bed and release of bacterial cells from the packed bed. These steps are shown in Fig. 2.

3.1. Comparing capture efficiency between chirped and straight IDTs

Prior uses of the ultrasonic nanosieve [44–47] employed chirped IDTs (Fig. 3a), which have a large number of finger pairs (N = 35) with varying widths and spacings to allow broadband operation. Here, we use straight IDTs (Fig. 3b) with a reduced number of finger pairs (N = 26) with a fixed width and pitch. This reduces the signal reflection coefficient significantly from (0.6 < S11 < 0.7) to (0.1 < S11 < 0.3), increasing the system efficiency and allowing for higher flow rates at a lower power regime. The only limitation of this new design is that our system can only operate a frequency of 70 MHz, which corresponds to the resonance frequency of the 15 μm microbeads. The microbeads size was selected due to their previously demonstrated high capture efficiency [46].

As shown in Fig. 3c, straight IDTs allowed for much higher capture efficiencies than chirped IDTs even at low power operation (0.5 W). To achieve a comparable level of efficiency with chirped IDTs powers 11 times higher (5.5 W) are required, and this can only be achieved after reducing the flow rate (see Fig. S1, in Supplementary Material). This enabled the use of much higher flow rates (up to 0.4 μL/min) while maintaining high capturing efficiency (95%), as seen in Fig. 3d. The small 5% decrease in capture efficiency is attributed to the larger fluid drag which begins to overcome the secondary Bjerknes force in the packed bed. In comparison, chirped IDTs performed extremely poorly, showing close to zero capture at flow rates over 0.1 μL/min.

3.2. Determining optimum parameters for bacteria capture

To determine optimum operating conditions for high-efficiency capture and release of bacterial cells, with and from the resonating packed bed, the straight IDTs were characterized for increasing flow rates, power, and concentrations. The system however is limited to a maximum flow rate of 0.5 μL/min as higher flow rates produced large hydraulic pressures within the packed bed which led to debonding of the PDMS channel.

As seen in Fig. 4a, when applying a power of 1.5 W, close to complete capture of cells was achieved even at the maximum flow rate of 0.5 μL/min. While this result validates the system's ability to concentrate at high flow rates for short durations of 30 s, it is expected that longer working times are required for concentration of highly diluted samples ($< 10^3$ CFU/mL). At long actuation durations and high powers, uncontrolled localized acoustothermal heating and evaporation of the fluid within the channel was observed. This disrupted the packed bed and decreased the efficiency of the nanosieve. Furthermore, it was observed that high powers rendered a lower release efficiency, likely due to the higher forces causing stronger attachment of cells to the polystyrene microparticles (Fig. 4b). To prevent these two drawbacks, the power was kept at 0.75 W and the flow rate was adjusted at 0.3 μL/min, which provided high capture and release efficiencies of 99% and 98%, respectively. Furthermore, when using these optimal parameters, without SAW activation, the percentage of undesired trapping of bacteria was an average of 10% (Fig. 4c). This low adhesion, which allowed for high concentration sample retrieval after ultrasonic concentration, was achieved by treating the channels and the microbeads surfaces using Pluronic F-127 [48]. Concentration and duration of surface treatment

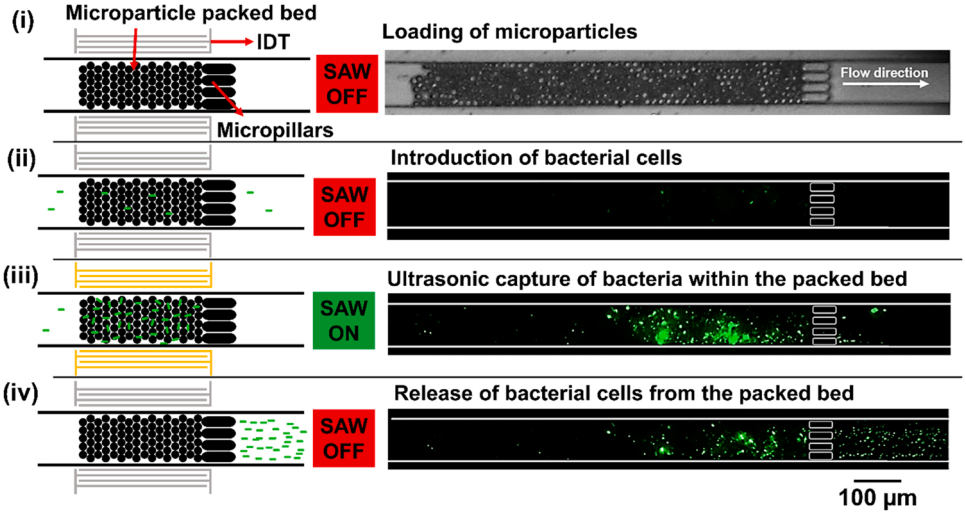

Fig. 2. Left: Illustration of the operating stages of the device. Right panel: Bright/fluorescence microscopy image of the packed bed at different operating stages with bacterial cells fluorescently labeled in green. (i) Loading of microparticles into the microfluidic channel. (ii) Introduction of bacterial cells (iii) Ultrasonic capturing of bacterial cells within the packed bed (SAW ON). (iv) Release of bacterial cells from the packed bed (SAW OFF) as a concentrated batch.

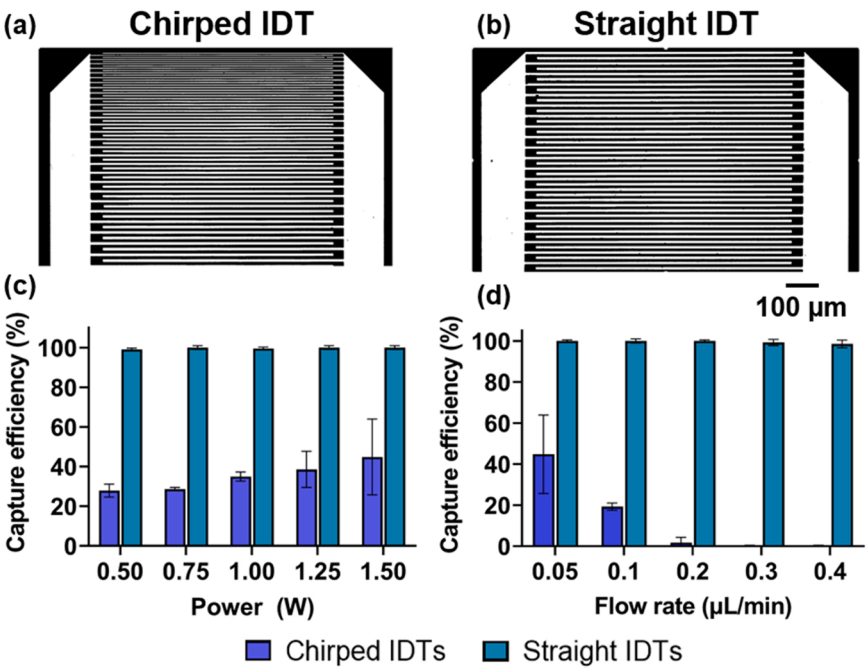

Fig. 3. Comparing the capture efficiency of chirped and straight IDTs. Experiments were set to a resonance frequency of 70 MHz, concentration of 5 × 10^5 CFU/mL, and ultrasonic activation duration of 30 s (a) Bright-field image of a single chirp IDT pair (varying finger width and spacing). (b) Bright-field image of a single straight IDT pair (constant finger width and spacing). (c) Capture efficiency with power for chirped against straight IDTs. (d) Capture efficiency with flow rate for chirped against straight IDTs. (All error bars for N = 5).

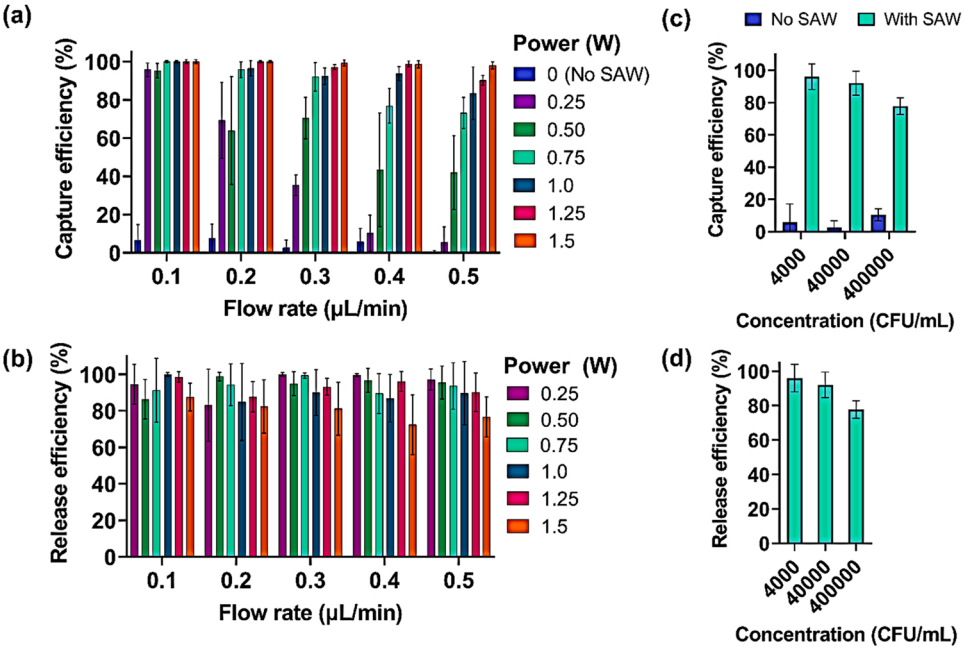

Fig. 4. Straight IDT characterization for bacteria cell capture and release efficiencies at 70 MHz for 30 s (a) Capture efficiency with increasing flow rate and power for an initial bacterial concentration of 4 x 10^5 CFU/mL. (b) Release efficiency with increasing flow rate and power. (c) Capture efficiency with increasing bacteria concentration with power fixed at 0.75 W and flow rate at 0.3 µL/min. "No SAW" refers to the bacteria captured just by the presence of the packed bed, without any acoustic activation. (d) Release efficiency with increasing bacteria concentration. (All error bars for N = 5).

was optimized to be 1% m/v for 1 h (see Fig. S2, in Supplementary Material). This surface treatment should also reduce the risk of non-specific binding, which can be useful for future use of the ultrasonic nanosieve with more complex biological matrices. Furthermore, as the capture efficiency of the system is largely dependent on the size and mechanical properties of the analyte and the microparticles constituting the packed bed [44–47], several sound wave activated nanosieves of varying pore diameters could be arranged for sequential separation and concentration of bacteria within more complex matrices.

When increasing the initial concentration of bacteria, it was observed that the capture efficiency decreased (Fig. 4c), due to the saturation of cells within the packed bed (weaker Bjerknes force as existing layers of bacteria increases distance of following cells from the microparticles). Similarly, release efficiency decreased significantly for highly concentrated samples (Fig. 4d). This decrease with increasing concentration is probably due to clustering of cells formed within the packed bed which are difficult to dislodge post-ultrasonic exposure. However, the system is designed for samples with much lower concentrations, where high efficiencies have been observed. Therefore, the optimal conditions at 0.75 W power using a flow rate of 0.3 µL/min were used in the following experiments. The viability of cells, determined from nucleic acid stains Syto-9 (total number of cells) and propidium iodide (dead cells only), was maintained at ~90% even at much higher powers (more than 6-fold) and longer exposure durations (up to 30 min), showing that system is highly biocompatible (See Fig. S3, in Supplementary Material).

3.3. Analysis using plate cultures and quantitative PCR

Standard plate cultures typically require large plating volumes of hundreds of microliters [9] to detect low concentrations of bacteria. However, samples that are not available in large volumes become challenging to detect as plating small volumes become unreliable due to a lack of colony formation at low bacterial concentrations. Standard plate cultures based on a low plating volume of 1 μL have a theoretical LOD of 10^3 CFU/mL (1 colony in 1 μL). Here, we used our system to concentrate bacteria samples with initial concentrations in the range of the LOD and an order of magnitude lower (~10^2 CFU/mL) to validate the capability of our system to enable the enumeration of colonies of bacteria in low concentration and small plating volumes of 1 μL without the need of culturing the sample for days.

Quantification of the initial concentration of bacteria prior was done via spectrophotometry. After 3 h of ultrasonic concentration, the system successfully increased the initial concentration from 5.5 × 10^3 CFU/mL to 2.76 x 10^4 CFU/mL (Fig. 5a). Similarly, a solution with the initial bacteria concentration of 5.5 x 10^2 CFU/mL (prior to ultrasonic concentration), which could not be detected by plate counting when using 1 μL, was increased 7-fold to 4.0 x 10^3 CFU/mL (Fig. 5b), enabling detection and quantification via this standard method.

By collecting samples at different stages of concentration it was possible to analyze the dynamic response of the system, as shown in Fig. 5c and d. For both concentrations, while the SAW was active, the counted colonies were under the LOD, further validating the high capturing efficiency of the system. Furthermore, the peak in concentration was observed 3 min after releasing the cells, indicating the optimal time for sample collection after the concentration step. To further validate the plate counting results, the enriched bacteria sample was analyzed via qPCR for genetic amplification of the 16 S rRNA gene. The enriched sample was compatible with this technique and exhibited close to an 8-fold increase in concentration, from 9.6 x 10^3 to 8.3 x 10^4 bacteria/mL. No significance was seen between the "Out-of-chip Control" and the "No SAW Control", further validating that cell loss within the device from undesired adhesion is low. The LOD of qPCR determined from standards (See Section 2.2, Quantitative PCR) was determined to be 2.67 x 10^3 CFU/mL, which is close to the selected starting bacteria concentration. These results demonstrate that the system is not only capable of enriching concentrations to enable plate counting but these enriched samples can be used in qPCR for specimen determination, even when the concentrations of the samples are close to the LOD.

3.4. Detection using fluorescence imaging with the ultrasonic nanosieve

Integration of fluorescence imaging and sensing is a growing field within microfluidics making compact, high-resolution imaging of biological samples possible [50]. Hence, developing strategies that integrate well with fluorescence imaging will enable a variety of portable, analytical microfluidic platforms. Beyond concentration to collect the sample and enable plate counting and PCR determination, our system also enables direct detection of bacteria on-chip by fluorescence measurements. This was done via sequential concentration and fluorescence imaging of cells as they are released from the packed bed after ultrasonic activation.

A range of concentrations, from 4 x 10^2 CFU/mL to 4 × 10^5 CFU/mL, were tested at different trapping durations to determine the optimal dynamic range for each of them (Fig. 6a). For an initial concentration of 4 × 10^5 CFU/mL, it was possible to detect the presence of bacteria after just 15 s of concentration. Conversely, for a low initial concentration of 4 x 10^2 CFU/mL, the minimum concentration time required was 16 min. The linear range of each concentration of bacteria was identified from the calibration plot. This enabled us to detect bacteria across different concentration ranges using optimal concentration times. For instance, for applications such as detection of foodborne pathogens *Salmonella* or *Campylobacter*, where it would be critical to identify these bacteria in the range between 10^3 and 10^5 CFU/mL (within the range of their infectious dose-the minimum number of pathogens to cause an infection) [3], it would be possible to operate the system with cycles of just 1 min of concentration, providing a LOD of 2 x 10^3 CFU/mL that enables fast monitoring and quantification of bacteria, as shown in Fig. 6b.

A main advantage of our device is the extreme flexibility to adapt its

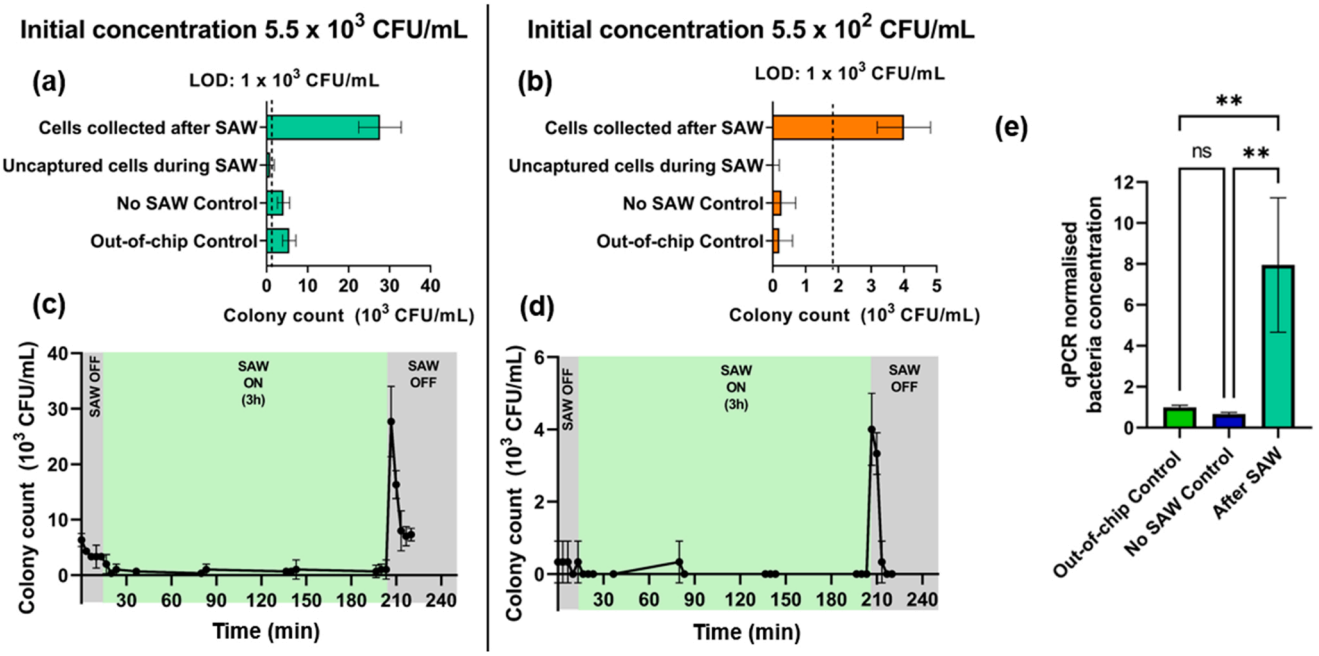

Fig. 5. Plate counting results before and after SAW activation for samples with initial bacteria concentration of (a) 5.5 x 10^3 CFU/mL and (b) 5.5 x 10^2 CFU/mL. Plate counting LOD for a 1 μL plating volume is denoted with a dashed line. "No SAW Control" represents the colony count of bacteria passing through the packed bed without surface acoustic wave activation. The "Out-of-chip Control" represents the original dilute bacteria sample. Concentration dynamics at the different stages of the concentration operation for samples with initial concentrations of (c) 5.5 x 10^3 CFU/mL and (d) 5.5 x 10^2 CFU/mL. (e) Quantitative PCR results showing 8-fold increase in concentration for concentration of bacterial cells with initial bacteria concentration of 9.55 x 10^3 CFU/mL for 3 h. (**: $P \leq 0.01$, ns: $P > 0.05$, $N = 3$).

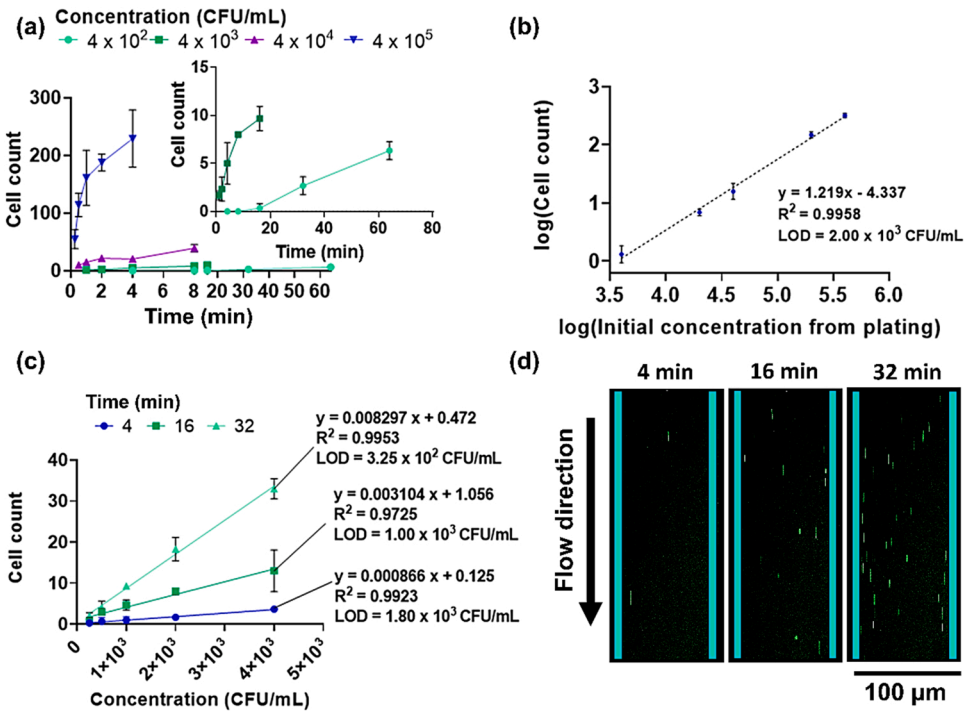

Fig. 6. Cell count from fluorescence counting. All experiments were performed at 0.75 W, 0.3 µL/min and 70 MHz. (a) Cell count from fluorescence imaging against time for concentrations ranging between 4×10^2 CFU/mL and 4×10^5 CFU/mL. Five durations of ultrasonic concentration were selected for each bacterial concentration tested. The durations selected depend on the initial concentration of the bacterial sample, with higher concentrations requiring shorter ultrasonic concentration times for detection (b) Calibration plot of log of cell count from fluorescence with 1 min of ultrasonic concentration against the log of known initial concentrations determined from colony counting for concentrations between 4 x 10^3 CFU/mL and 4×10^5 CFU/mL. (c) Calibration plot of cell count from fluorescence against known initial concentrations determined from colony counting for concentrations between 2.5 x 10^2 to 4 x 10^3 CFU/mL for varying concentration durations of 4 min, 16 min and 32 min (d) Fluorescence imaging of cells released downstream after varying ultrasonic exposure durations for initial bacterial concentration of 4 x 10^3 CFU/mL. (All error bars for N = 5).

sensing capabilities. By simply increasing the concentration time, it is possible to fine-tune the system's sensitivity and LOD. This was demonstrated by obtaining calibration plots for three longer concentration durations of 4, 16, and 32 min, as shown in Fig. 6c, with examples of the fluorescent images obtained seen in Fig. 6d. This enabled rapid detection of concentrations well below 10^3 CFU/mL, with increased sensitivity and an optimal LOD of 3.25×10^2 CFU/mL in just 32 min of concentration time, requiring an initial sample volume of only 10 µL. When less restrictive LODs are required, over 10^3 CFU/mL, the time required for detection is reduced to 4 min and the required volume is of only 1.2 µL. These results demonstrate the capability of our system to rapidly detect the presence of very small concentrations of bacteria in min without the need for cell culturing or extended plate counting experiments with improved LOD, demonstrating that the microfluidic ultrasonic nanosieve is a strong candidate for continuous detection of bacteria samples with low concentrations and small sample volumes. (All error bars for N = 5).

4. Conclusions

The ultrasonic nanosieve was used to concentrate and detect bacterial cells at low initial concentrations and small sample volumes for the first time. Straight IDTs were implemented to enable 3-fold higher working flow rates at a much lower power regime whilst still maintaining capturing efficiencies of 99%. This approach enabled the use of standard plate counting and qPCR for quantification of cells on samples initially below the LOD using small 1 µL plating volumes. Furthermore, our system allowed for rapid detection of bacteria in-chip across a wide range of concentrations, achieving a LOD as low as 3.25×10^2 CFU/mL in just 32 min with only 10 µL of original sample. These show that the device is easily integrated with other cell-counting techniques in both microfluidic and non-microfluidic platforms. It is worth noting, that although only *E. coli* bacteria cells were tested in this work, most common bacteria genera are still within the same dimension range (a few microns), hence, mechanically, the device would perform similarly in its capture efficiency. Overall, the system proves as a competitive candidate for continuous low concentration bacteria monitoring with a large potential for future upscaling.

CRediT authorship contribution statement

Bryan Ang: Conceptualization, Methodology, Validation, Formal analysis, Investigation, Data curation, Writing – original draft, Visualization. **Ruhollah Habibi**: Conceptualization, Methodology, Writing – review & editing. **Ciaren Kett**: Validation, Formal analysis, Investigation, Data curation, Writing – original draft. **Wai Hoe Chin**: Resources, Writing – review & editing. **Jeremy Barr**: Resources, Writing – review & editing, Supervision. **Kellie L. Tuck**: Conceptualization, Resources, Writing – review & editing, Supervision, Project administration. **Adrian Neild**: Conceptualization, Methodology, Resources, Writing – review & editing, Supervision, Project administration, Funding acquisition. **Victor J. Cadarso**: Conceptualization, Methodology, Resources, Writing – review & editing, Supervision, Project administration, Funding acquisition.

Declaration of Competing Interest

The authors declare that they have no known competing financial interests or personal relationships that could have appeared to influence the work reported in this paper.

Data availability

Data will be made available on request.

Acknowledgments

This work was performed in part at the Melbourne Centre for Nanofabrication (MCN) in the Victorian Node of the Australian National Fabrication Facility (ANFF). The authors thank Citsabehsan Devendran for advice on fabrication and experimental protocol development and Mateo Villate for surface treatment protocol optimization and graphic modeling.

Appendix A. Supporting information

Supplementary data associated with this article can be found in the

online version at doi:10.1016/j.snb.2022.132769.

References

[1] L. Castillo-Henríquez, M. Brenes-Acuña, A. Castro-Rojas, R. Cordero-Salmerón, M. Lopretti-Correa, J.R. Vega-Baudrit, Biosensors for the detection of bacterial and viral clinical pathogens, Sens. (Basel) 20 (2020) 6926.

[2] D.-K. Kang, M.M. Ali, K. Zhang, S.S. Huang, E. Peterson, M.A. Digman, et al., Rapid detection of single bacteria in unprocessed blood using Integrated Comprehensive Droplet Digital Detection, Nat. Commun. 5 (2014) 5427.

[3] P. Leonard, S. Hearty, J. Brennan, L. Dunne, J. Quinn, T. Chakraborty, et al., Advances in biosensors for detection of pathogens in food and water, Enzym. Microb. Technol. 32 (2003) 3–13.

[4] J.W.-F. Law, N.-S. Ab Mutalib, K.-G. Chan, L.-H. Lee, Rapid methods for the detection of foodborne bacterial pathogens: principles, applications, advantages and limitations, Front. Microbiol. 5 (2015).

[5] C. Giuliano, C.R. Patel, P.B. Kale-Pradhan, A guide to bacterial culture identification and results interpretation, P T 44 (2019) 192–200.

[6] O. Lazcka, F.J.D. Campo, F.X. Muñoz, Pathogen detection: A perspective of traditional methods and biosensors, Biosens. Bioelectron. 22 (2007) 1205–1217.

[7] C. Wang, F. Madiyar, C. Yu, J. Li, Detection of extremely low concentration waterborne pathogen using a multiplexing self-referencing SERS microfluidic biosensor, J. Biol. Eng. 11 (2017) 9.

[8] J.-C. Lagier, S. Edouard, I. Pagnier, O. Mediannikov, M. Drancourt, D. Raoult, Current and past strategies for bacterial culture in clinical microbiology, Clin. Microbiol. Rev. 28 (2015) 208–236.

[9] U.S.EPA, Method 1611: Enterococci in water by TaqMan® quantitative polymerase chain reaction (qPCR) assay, EPA-821-R-12–008, 2012: 15–17.

[10] S. Aboutalebian, K. Ahmadikia, H. Fakhim, J. Chabavizadeh, A. Okhovat, M. Nikaeen, et al., Direct Detection and Identification of the Most Common Bacteria and Fungi Causing Otitis Externa by a Stepwise Multiplex PCR, Front. Cell. Infect. Microbiol. 11 (2021).

[11] A. Rompré, P. Servais, J. Baudart, M.-R. de-Roubin, P. Laurent, Detection and enumeration of coliforms in drinking water: current methods and emerging approaches, J. Microbiol. Methods 49 (2002) 31–54.

[12] K.M. Tuohy, R.K. Finlay, A.G. Wynne, G.R. Gibson, A Human Volunteer Study on the Prebiotic Effects of HP-Inulin—Faecal Bacteria Enumerated Using Fluorescent In Situ Hybridisation (FISH), Anaerobe 7 (2001) 113–118.

[13] C. Moss, D.H. Green, B. Pérez, A. Velasco, R. Henríquez, J.D. McKenzie, Intracellular bacteria associated with the ascidian Ecteinascidia turbinata: phylogenetic and in situ hybridisation analysis, Mar. Biol. 143 (2003) 99–110.

[14] C. Morris, Y.S. Lee, S. Yoon, Adventitious agent detection methods in bio-pharmaceutical applications with a focus on viruses, bacteria, and mycoplasma, Curr. Opin. Biotechnol. 71 (2021) 105–114.

[15] S.L.R. Ellison, C.A. English, M.J. Burns, J.T. Keer, Routes to improving the reliability of low level DNA analysis using real-time PCR, BMC Biotechnol. 6 (2006) 33.

[16] A. Tsuru, T. Setoguchi, N. Kawabata, M. Hirotsu, T. Yamamoto, S. Nagano, et al., Enrichment of bacteria samples by centrifugation improves the diagnosis of orthopaedics-related infections via real-time PCR amplification of the bacterial methicillin-resistance gene, BMC Res Notes 8 (2015) 288.

[17] X. Qian, R.V. Lloyd, Recent developments in signal amplification methods for in situ hybridization, Diagn. Mol. Pathol. 12 (2003).

[18] S. Kay, G. Van den Eede, The limits of GMO detection, Nat. Biotechnol. 19 (2001) 405.

[19] S.N. Peirson, J.N. Butler, R.G. Foster, Experimental validation of novel and conventional approaches to quantitative real-time PCR data analysis, Nucleic Acids Res. 31 (2003) e73-e73.

[20] S. Lin, Z. Cheng, Q. Li, R. Wang, F. Yu, Toward Sensitive and Reliable Surface-Enhanced Raman Scattering Imaging: From Rational Design to Biomedical Applications, ACS Sens. 6 (2021) 3912–3932.

[21] G. Xing, W. Zhang, N. Li, Q. Pu, J.-M. Lin, Recent progress on microfluidic biosensors for rapid detection of pathogenic bacteria, Chin. Chem. Lett. (2021).

[22] H.-J. Kim, S.-J. Choi, Rapid single-cell detection of pathogenic bacteria for in situ determination of food safety, Anal. Methods 12 (2020) 5621–5627.

[23] D.A. Boehm, P.A. Gottlieb, S.Z. Hua, On-chip microfluidic biosensor for bacterial detection and identification, Sens. Actuators B: Chem. 126 (2007) 508–514.

[24] N. Beyor, T.S. Seo, P. Liu, R.A. Mathies, Immunomagnetic bead-based cell concentration microdevice for dilute pathogen detection, Biomed. Micro 10 (2008) 909.

[25] F. Huang, R. Guo, L. Xue, G. Cai, S. Wang, Y. Li, et al., An Acid-Responsive Microfluidic Salmonella Biosensor Using Curcumin as Signal Reporter and ZnO-Capped Mesoporous Silica Nanoparticles for Signal Amplification, Sens. Actuators B: Chem. 312 (2020), 127958.

[26] M. Majdinasab, A. Hayat, J.L. Marty, Aptamer-based assays and aptasensors for detection of pathogenic bacteria in food samples, TrAC Trends Anal. Chem. 107 (2018) 60–77.

[27] V.C. Ozalp, G. Bayramoglu, Z. Erdem, M.Y. Arica, Pathogen detection in complex samples by quartz crystal microbalance sensor coupled to aptamer functionalized core–shell type magnetic separation, Anal. Chim. Acta 853 (2015) 533–540.

[28] G. Bayramoglu, V.C. Ozalp, M. Oztekin, M.Y. Arica, Rapid and label-free detection of Brucella melitensis in milk and milk products using an aptasensor, Talanta 200 (2019) 263–271.

[29] A.D. Dursun, B.A. Borsa, G. Bayramoglu, M.Y. Arica, V.C. Ozalp, Surface plasmon resonance aptasensor for Brucella detection in milk, Talanta 239 (2022), 123074.

[30] H. Han, B. Sohn, J. Choi, S. Jeon, Recent advances in magnetic nanoparticle-based microfluidic devices for the pretreatment of pathogenic bacteria, Biomed. Eng. Lett. 11 (2021) 297–307.

[31] S. Podszun, P. Vulto, H. Heinz, S. Hakenberg, C. Hermann, T. Hankemeier, et al., Enrichment of viable bacteria in a micro-volume by free-flow electrophoresis, Lab a Chip 12 (2012) 451–457.

[32] M.F. Kamuri, Z. Zainal Abidin, M.H. Yaacob, M.N. Hamidon, N.A. Md Yunus, S. Kamarudin, Separation and Detection of Escherichia coli and Saccharomyces cerevisiae Using a Microfluidic Device Integrated with an Optical Fibre, Biosensors 9 (2019).

[33] A. Ozcelik, J. Rufo, F. Guo, Y. Gu, P. Li, J. Lata, et al., Acoustic tweezers for the life sciences, Nat. Methods 15 (2018) 1021–1028.

[34] K.A. Stevens, L.-A. Jaykus, Bacterial separation and concentration from complex sample matrices: a review, Crit. Rev. Microbiol. 30 (2004) 7–24.

[35] J. Gai, E. Dervisevic, C. Devendran, V.J. Cadarso, M.K. O'Bryan, R. Nosrati, et al., High-frequency ultrasound boosts bull and human sperm motility, Adv. Sci. 9 (2022), 2104362.

[36] C. Devendran, J. Carthew, J.E. Frith, A. Neild, Cell adhesion, morphology, and metabolism variation via acoustic exposure within microfluidic cell handling systems, Adv. Sci. 6 (2019), 1902326.

[37] J. Gai, R. Nosrati, A. Neild, High DNA integrity sperm selection using surface acoustic waves, Lab a Chip 20 (2020) 4262–4272.

[38] P. Zhang, H. Bachman, A. Ozcelik, T.J. Huang, Acoustic microfluidics, Annu. Rev. Anal. Chem. 13 (2020) 17–43.

[39] A.G. Guex, N. Di Marzio, D. Eglin, M. Alini, T. Serra, The waves that make the pattern: a review on acoustic manipulation in biomedical research, Mater. Today Bio 10 (2021), 100110.

[40] C. Richard, A. Neild, V.J. Cadarso, The emerging role of microfluidics in multi-material 3D bioprinting, Lab a Chip 20 (2020) 2044–2056.

[41] T. Laurell, F. Petersson, A. Nilsson, Chip integrated strategies for acoustic separation and manipulation of cells and particles, Chem. Soc. Rev. 36 (2007) 492–506.

[42] A. Garcia-Sabaté, A. Castro, M. Hoyos, R. González-Cinca, Experimental study on inter-particle acoustic forces, J. Acoust. Soc. Am. 135 (2014) 1056–1063.

[43] T. Baasch, I. Leibacher, J. Dual, Multibody dynamics in acoustophoresis, J. Acoust. Soc. Am. 141 (2017) 1664–1674.

[44] R. Habibi, C. Devendran, A. Neild, Trapping and patterning of large particles and cells in a 1D ultrasonic standing wave, Lab a Chip 17 (2017) 3279–3290.

[45] R. Habibi, A. Neild, Sound wave activated nano-sieve (SWANS) for enrichment of nanoparticles, Lab a Chip 19 (2019) 3032–3044.

[46] R. Habibi, V. He, S. Ghavamian, A. de Marco, T.-H. Lee, M.-I. Aguilar, et al., Exosome trapping and enrichment using a sound wave activated nano-sieve (SWANS), Lab a Chip 20 (2020) 3633–3643.

[47] R. Habibi, A. Neild, Nanoparticle Capture Using Ultrasonic Actuation, 2019 20th International Conference on Solid-State Sensors, Actuators and Microsystems & Eurosensors XXXIII (TRANSDUCERS & EUROSENSORS XXXIII)2019, pp. 797–800.

[48] V.N. Luk, G.C.H. Mo, A.R. Wheeler, Pluronic Additives: A Solution to Sticky Problems in Digital Microfluidics, Langmuir 24 (2008) 6382–6389.

[49] C. Lee, S. Lee, S.G. Shin, S. Hwang, Real-time PCR determination of rRNA gene copy number: absolute and relative quantification assays with Escherichia coli, Appl. Microbiol. Biotechnol. 78 (2008) 371–376.

[50] E.J. Vargas-Ordaz, S. Gorelick, H.M. York, B. Liu, M.L. Halls, S. Arumugam, et al., Three-dimensional imaging on a chip using optofluidics light-sheet fluorescence microscopy, Lab a Chip 21 (2021) 2945–2954.

Bryan Ang received a Bachelor's in Mechanical Engineering from Monash University Australia, in 2018. He is currently a PhD student at Monash University Australia under the Department of Mechanical and Aerospace Engineering. His research interests include microbiological sensing systems for water and food using microfluidics and acoustics.

Ruhollah Habibi Graduated from Sharif University of Technology (Iran's top engineering school), Ruhollah worked in the general industry for an extended period up to 2016. Already accomplished handling various scale projects in roles of design, technical support, project engineering and project management both within Australia and internationally, he decided to return to research, where he completed his PhD at Monash University Australia in 2020. His research interests include underlying mechanisms of acoustophoresis, with a special focus on the secondary interaction between particles, enabling Lab-on-Chip platforms for particle/cell manipulation within microfluidic systems exploiting the contactless nature of acoustic forces. He currently holds a position as a Technical Support Lead at Callidus Process Solutions.

Ciaren Kett holds a Bachelor of Science in Genetics & Molecular Biology from Monash University. In 2021 she graduated from her Master of Biotechnology from Monash University and The Australian Regenerative Medicine Institute (ARMI). Ciaren then worked as a Research Assistant in The Barr Lab at The School of Biological Sciences, Monash University where she used a gut-on-a-chip device to track bacteriophage and microbial dynamics. She is currently a Clinical Scientist at 360biolabs, where she works across the Molecular and Virology teams.

Wai Hoe Chin obtained his Bachelors with First Honours in Biomedical Sciences at the The University of Edinburgh, United Kingdom. Subsequently, he obtained his PhD in Microbiology from Monash University, Australia in 2022. He is currently a postdoctoral scholar at the Department of Biology in San Diego State University, United States. His current

research involves bacteriophage biology and dynamics in vivo with the aim to develop better clinical strategies for effective phage therapy against bacterial infections.

Jeremy Barr completed his PhD in microbiology at The University of Queensland in 2011. He then moved to San Diego, USA to complete a postdoctoral position with Prof. Forest Rohwer at San Diego State University. While there he studied the interactions of bacteriophage with mucosal surfaces and was involved in a word-first phage therapy case treating a patient with disseminated, multidrug-resistant infection. In 2016, he joined Monash University's School of Biological Sciences where he is currently a Senior Lecturer and Group Leader. His research group studies bacteriophages and their tripartite interactions with their bacterial hosts and the human body. In 2020, he joined the Centre to Impact AMR where he leads translational phage therapy work.

Kellie Tuck A/Professor Kellie Tuck obtained her PhD from the University of Adelaide. After postdoctoral research positions at the University of South Australia, Australia, and the University of Cambridge, UK she returned to Australia where she took up an academic position at the School of Chemistry, Monash University, Australia. Her research focuses on the development of sensors for a variety of applications, as well as the synthesis of bioactive compounds with potential therapeutic applications. She is engaged in a number of interdisciplinary research programs that combine organic chemistry with analytical chemistry, chemical engineering, and/or microbiology.

Adrian Neild received a PhD in engineering from the University of Warwick, in 2003. Subsequently, he worked as a postdoctoral researcher at the Institute for Mechanical Systems at ETH Zurich (Swiss Federal Institute of Technology Zurich). He has been a faculty member at Monash University since 2006 and is currently a Professor and Deputy Dean for strategic Initiatives in the Faculty of Engineering. His research interests are in the field of microsystems, specialising in microfluidics for multidisciplinary research.

Dr. Victor Cadarso received a PhD in Physics in Dec 2008 from the Autonomous University of Barcelona. He conducted his research in the Chemical Transducers Group (GTQ) at the Institute of Microelectronics of Barcelona (IMB) in the frame of Micro and Nanotechnology for the development of microsystems and (bio)sensors. In 2009 he joined the Swiss Federal Institute of Technology, Lausanne (EPFL) as a Marie Curie Fellow. In 2013 he obtained an Ambizione Fellowship from the Swiss National Science foundation, to join the Laboratory for Micro and Nanotechnology at the Paul Scherrer Insitut (PSI). In 2016 he joined the Department of Mechanical and Aerospace Engineering in Monash University as Senior Lecturer to establish a laboratory in the frame of micro and nanotechnologies, sensing and imaging applications, soft matter and surface modification for biomedical and environmental applications. He has been also appointed as Research Leader for the Centre to Impact Antimicrobial Resistance.